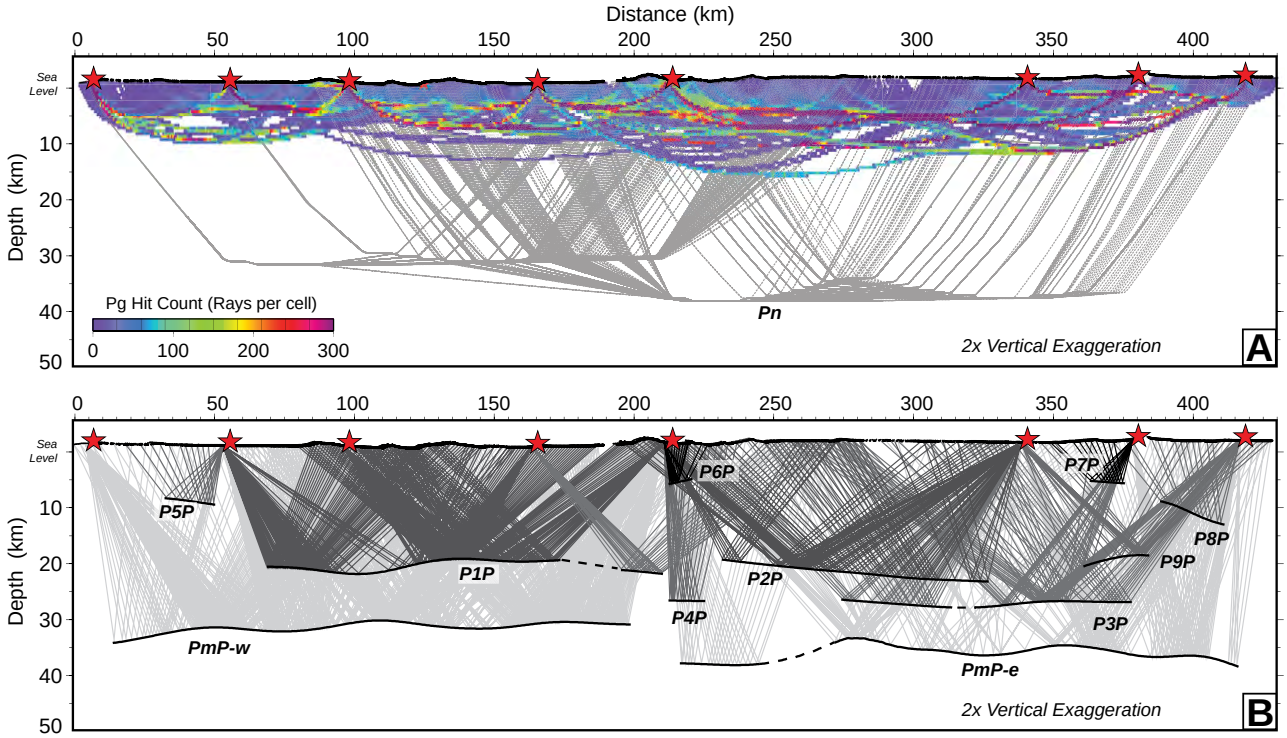

Figure 7. Ray coverage of turning, reflected, and refracted phases in the final velocity model. (A) Upper-crustal turning rays (Pg) are illustrated by hit count in 0.5 km grid cells. Every tenth ray is shown for the upper-mantle refraction Pn (gray). (B) Every fifth ray is shown for reflections from the Moho (PmP, light gray) and for reflections P1P to P9P (dark gray). See text for description of the labeled seismic arrivals.

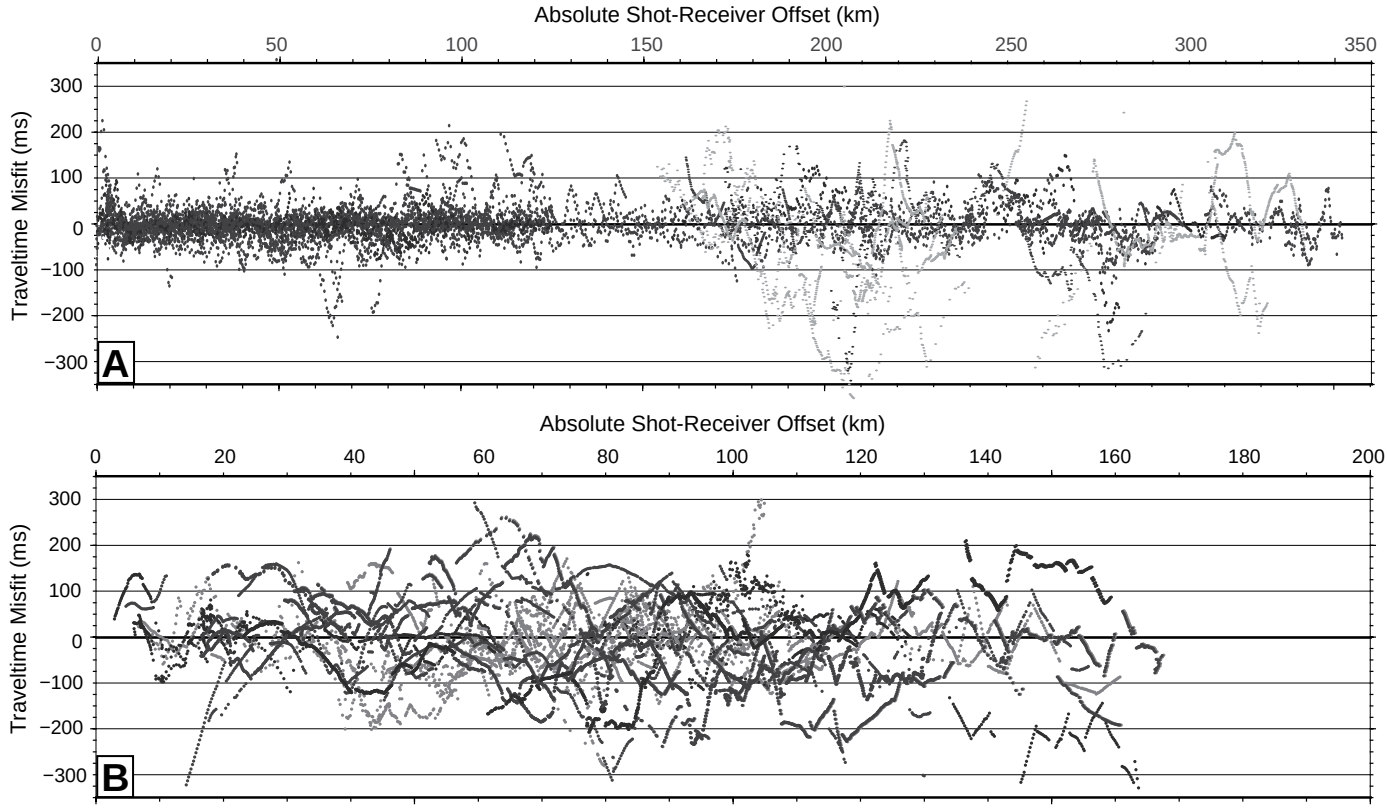

Figure 8. Misfit between picked and calculated traveltimes. (A) Refracted phases; Pg (black), Pn (gray). (B) Reflected phases (see Fig. 7B). Misfit details are in Table 1.

including longer offsets, was improved from >60 ms without the high-resolution near-surface layer.

A nongeologic 2-D boundary was extracted from near the bottom of the reliable Pg ray coverage, near 10 km subsurface depth. The model above this boundary was held fixed when modeling the deeper crust. The velocities at this boundary were extended to greater depth and smoothed to produce the starting model for the middle crust.

Middle Crust and Reflectors

Once the upper-crust velocity was well resolved, wide-angle reflection traveltimes from the midcrust were used to invert for reflector depth and velocity structure between the fixed upper crust and the reflector. Velocity was primarily constrained by the curvature of the reflected arrival times, so phases observed over a long-offset range had little trade-off between depth and the velocity of the overlying layer. This resolution was improved when the reflected phase was observed on more than one shot.

Reflection traveltimes were initially inverted for the best-fitting constant reflector depth in the extended Pg velocity model. Next, the reflection was forward modeled using a range of constant velocities, starting with the velocity at the base of the overlying Pg model and increasing in 0.1 km/s increments until the misfits stopped improving and began to deteriorate. This velocity model was then used to invert for reflector depth, and the process was repeated until a best-fitting combination of constant velocity and constant depth was found. For a shallowly dipping reflector, an incorrect average velocity produces misfits that are strongly dependent upon distance. This pattern allows the average depth and overlying velocity of reflectors observed over a long range of offsets and/or on multiple shots to be well constrained. The best velocity and depth combination for each reflector was used as the starting model for the 2-D inversion.

Reflection traveltimes were inverted for laterally varying reflector depth in this best-fitting starting velocity model, and then for 2-D velocity between the reflector and the overlying fixed layer, and then again for reflector depth (Zelt et al., 1996). Reflector depth was smoothed horizontally during the inversion to maintain geologically reasonable structures and eliminate topography that is not required by the data. For most of the reflected phases from the midcrust, the reflectors were smoothed 10–20 km horizontally to incorporate ray paths from multiple shots (Fig. 7B; Table 1). However, across the Idaho batholith, they were smoothed 40–60 km horizontally due to the gap in shot coverage. Velocity in the layers above the reflectors and below the shallower fixed layer was smoothed 20–60 km in *x*, with larger smoothing used for deeper layers and larger shot offsets, 3 km in *z*, and forced to be constant in *y*. Where multiple midcrustal reflectors were observed, reflector depth and velocity were determined for the shallower reflector first, and then this structure was fixed to model the deeper reflection traveltimes. While the ray coverage on the reflectors is good (Fig. 7B), traveltime misfits of 200–300 ms (Fig. 8B; Table 1) represent probable cycle skips.

Most of the crustal reflections observed on the IDOR shots do not have associated refractions from beneath the reflector, so there are not well-constrained velocity contrasts across any of the reflectors. The high-amplitude reflection recorded on the western end of the line probably has an associated refracted phase, but modeling indicates this phase would never emerge as a first arrival, so it is probably hidden in the coda of the earlier arrivals. The reflections without associated refractions were modeled as "floating" reflectors (Zelt, 1999). Although seismic energy can be reflected back to the surface due to the impedance contrast between two layers with different bulk properties (seismic velocity and/or density), reflections may also result from the layering of thin beds, sills, or shear fabrics. These reflections do not require a change in bulk properties across the reflection surface, and therefore midcrustal reflections are modeled as "floating" within a smooth velocity gradient unless a refraction is observed from beneath the reflector, or deeper data require much higher velocity beneath the reflector. For most of these reflectors, the deeper data allow at most a small velocity contrast across the reflector, such that the next layer's average velocity is the same. Exceptions to these average velocities occurred in the lower crust on either side of the line.

The strong, deep P1P reflector beneath the western end of the line implies a velocity contrast based on the reflector strength on shots 2, 3, and 5 (Fig. 3; Data Repository Fig. S1A[1]). The underlying Moho PmP reflection is not observed over a very long offset range, so velocity beneath the P1P reflector is not well constrained by this shot. However, the difference in curvature between the P1P and PmP arrivals observed on multiple shots implies a different average velocity above each reflector, indicating a higher-velocity layer must exist between the two reflectors. The velocity assigned to this layer is the minimum average velocity required to match the data.

On the eastern end of the line, the P2P and P3P reflections have very similar curvature, indicating there is not a strong velocity contrast between these reflectors. The curvature of the PmP reflection is different from that of P2P and P3P, and it requires a higher velocity in the lower crust between P3P and the Moho. East of shot 7, the difference in curvature between the P2P and PmP reflections requires a higher velocity in the lower crust, which is consistent with the westward extrapolation of the P3P velocity discontinuity. However, the shot gap, missing stations, and complexities across the WISZ disrupt the continuity of arrivals in this area, preventing this reflector from being identified farther west. The same average velocity can be achieved with a smooth gradient from the P2P reflector to the Moho, which is also consistent with the data, so the velocity discontinuity was restricted to the region beneath the P3P reflector, and the remaining lower crust was modeled with a gradient.

Lower Crust, Moho, and Uppermost Mantle

Once all of the midcrustal reflectors were fixed in place, the velocity structure above those reflectors was fixed, and the PmP phase reflected from the Moho was incorporated into the model. The initial ray path calculations indicated significant variability in the Moho depth, and smoothing the Moho beneath the entire seismic line resulted in severe velocity artifacts. To isolate the source of the artifacts, PmP arrivals from each shot were inverted independently for reflector depth. Based on these reflector depths, the Moho reflections were divided into two separate phases, PmP-w and PmP-e. Traveltimes from shots 1, 2, 3, 5, and 7-west were designated PmP-w, and traveltimes from shots 7-east, 8, 9, and 10 were designated PmP-e. These reflectors were modeled independently.

The ray coverage at the Moho on the western side (PmP-w) is dense for most of the model (Fig. 7B). The PmP-e ray coverage on the eastern side is sparser, with modest coverage and higher estimated picking errors beneath the Idaho batholith. Due to the shot distribution on the east and the shadow-zone effect for shots from the west, the western end of the PmP-e reflector is only constrained by the short-offset PmP arrivals from shot 7. This relatively low-amplitude arrival is clearly visible behind the high-amplitude midcrust P4P reflection (Fig. 4).

Inversion for reflector depth and lower-crustal velocity followed the same procedures as for the shallower reflectors. The Moho on the western side of the line is better constrained due to smaller shot spacing and higher-amplitude PmP-w reflections. Traveltime misfits for the lower crust above the PmP-w reflector are ~107 ms. The PmP-e reflector is less

[1]GSA Data Repository Item 2017082, Figure S1, example of the model region constrained by a reflected phase, is available at http://www.geosociety.org/datarepository/2017, or on request from editing@geosociety.org.

well constrained due to the shot gap across the batholith and near-surface complexities from the shots in the Basin and Range. In the area of the batholith, average misfits are ~180 ms, indicating probable cycle skips due to the lack of reciprocity in this area. On the eastern end, misfits are ~220 ms (Fig. 8B; Table 1).

Once the crustal velocity model and Moho depth were fixed, Pn arrivals were inverted for velocity in the uppermost mantle lid (Data Repository Fig. S1B). The limited range of geologically feasible velocities in the uppermost mantle means the Pn phase also serves to verify the crustal velocity model and Moho depth. The Pn arrivals on shots 1, 2, and 3 have good signal quality. Pn phases are observed on the other shots (except shot 9), but the signal-to-noise ratio is not as high, so the picking uncertainty is greater for these arrivals (Table 1). Pn traveltimes calculated through the final velocity model using a constant 8.0 km/s uppermost mantle velocity provide a good fit for the observed Pn phases at less than ~220 km offset on all shots. Longer-offset Pn arrivals are difficult to identify on most shots. A very large smoothing was utilized to invert for velocity in the uppermost mantle, which did not vary significantly from 8.0 km/s.

Seismic Velocity Model

The whole-crust seismic velocity model produced from the IDOR controlled-source data reveals a strong contrast in seismic properties beneath the WISZ (Figs. 9 and 10). The western half of the line is characterized by faster velocities throughout the entire crust, while the eastern side has slower velocities (Figs. 9 and 10). These velocities are consistent with those measured by Christensen and Mooney (1995) and Christensen (1996) under laboratory conditions for intermediate-to-mafic and felsic compositions, respectively. In addition, there is a large, steep step on the Moho beneath and slightly east of the WISZ. These structures indicate the presence of a boundary that coincides with the surface expression of the WISZ.

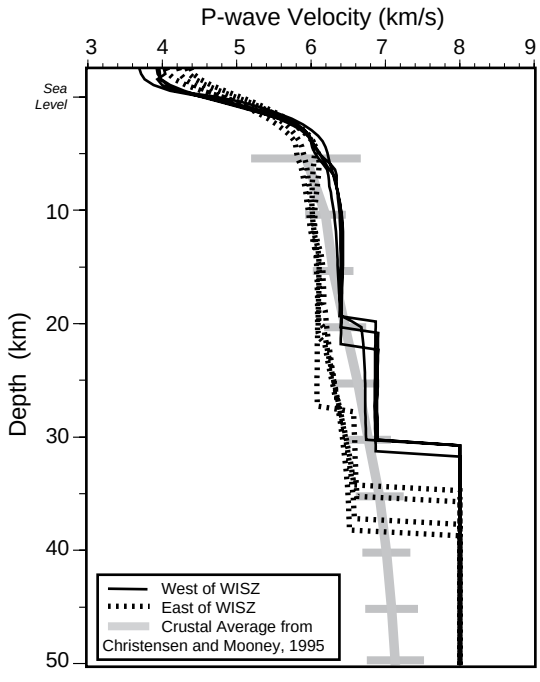

Figure 9. Comparison of vertical profiles through the velocity model of Figure 10 at model km 50–400 in 50 km intervals. Solid lines are profiles west of the western Idaho shear zone (WISZ); dashed lines are east of the WISZ. Gray line is crustal average velocity from Christensen and Mooney (1995).

On the western and central portions of the line, there are several small, surface low-velocity bodies that are modeled using the short-offset Pg traveltimes recorded on densely deployed stations (Fig. 10). These correlate with Cenozoic sediment-filled basins identified at the surface (Fig. 1). The eastern end of the profile also reveals sediment-filled basins, but these Basin and Range–related fault-bounded basins are less well resolved due to significant local north-south geologic variation and a lower signal-to-noise ratio.

Below ~5 km depth on the western half of the profile in the accreted terranes, velocities of 6.3–6.5 km/s in the middle crust (Figs. 9 and 10) are consistent with rocks of felsic to intermediate composition (Christensen and Mooney, 1995). The very high-amplitude P1P reflection observed on the western shots (Figs. 3 and 4) indicates a boundary at 21–22 km subsurface depth (~20 km below sea level), 8–10 km above the Moho (Fig. 10). The lower crust beneath the reflector did not produce a first-arrival refraction, but the relative curvatures of the P1P reflection and the PmP phase reflected from the Moho constrain the layer to 6.8 ± 0.1 km/s. The fastest portion of this layer corresponds to the highest-amplitude section of the reflector (Fig. 3) and the thinnest crust (Fig. 10), strongly suggesting a discontinuity across the boundary. This velocity is interpreted as evidence of a mafic lower crust (Christensen and Mooney, 1995). Another smaller-amplitude reflection, P5P, is west of shot 2 at ~10 km subsurface depth. It has limited lateral extent and cannot be shown to correspond to a velocity contrast and thus has been modeled as a "floating" reflector.

On the eastern half of the profile, the seismic velocity in the upper 24–30 km of the crust is ≤6.2 km/s, which is consistent with a felsic lithology (Christensen and Mooney, 1995). The upper 10 km is ≤6.0 km/s, except in a region of slightly faster velocity at 5–8 km depth from model km 270 to 325 (Fig. 10). In this area, a slightly faster velocity of 6.2–6.3 km/s is required by the data, based on velocity tests, but this is in the region of poorest ray coverage due to the shot gap and fire-related station gap (Fig. 7), so it is heavily smoothed. With the exception of this feature, there is little velocity difference between the Idaho batholith and the Precambrian craton to the east.

A continuous reflector, P2P, is observed on shots 7 and 8 (Figs. 4 and 5), which are reversed across the batholith. This phase corresponds to a reflector at 20–24 km subsurface depth, dipping gently to the east (Fig. 10). A deeper reflector, P3P, is observed on shots 8, 9, and 10 and overlaps laterally with the P2P reflector. This reflector is at ~29 km subsurface depth, 8–10 km above the Moho (Fig. 10). The seismic velocity below the P3P reflector is 6.6 ± 0.1 km/s, constrained by curvature of the P3P and PmP reflectors. This velocity is consistent with that of intermediate-composition rocks at lower-crustal pressures and temperatures (Christensen and Mooney, 1995). The western end of P3P is not constrained by shot 7 due to shot and receiver gaps and data quality, so it is possible this reflector could extend further west. There is no evidence in the data for an extension, but there is also not clear evidence of the reflector's termination. The curvature of the P2P and underlying PmP reflectors is consistent with either a westward extension of the velocities above and below the P3P reflector, or a smooth gradient with an equivalent average velocity (Fig. 10). A strong, short P4P reflector exists immediately east of the WISZ at ~27 km subsurface depth (Fig. 10). Velocity below this reflector, in the lower-crustal corner near the WISZ, is not well constrained, but it is inconsistent with mantle velocity. Several shallow reflectors underlie the eastern half of the line, but none requires an associated large increase in velocity.

The Moho was modeled independently on the east and west sides of the profile to avoid artificially imposing structure when it became apparent

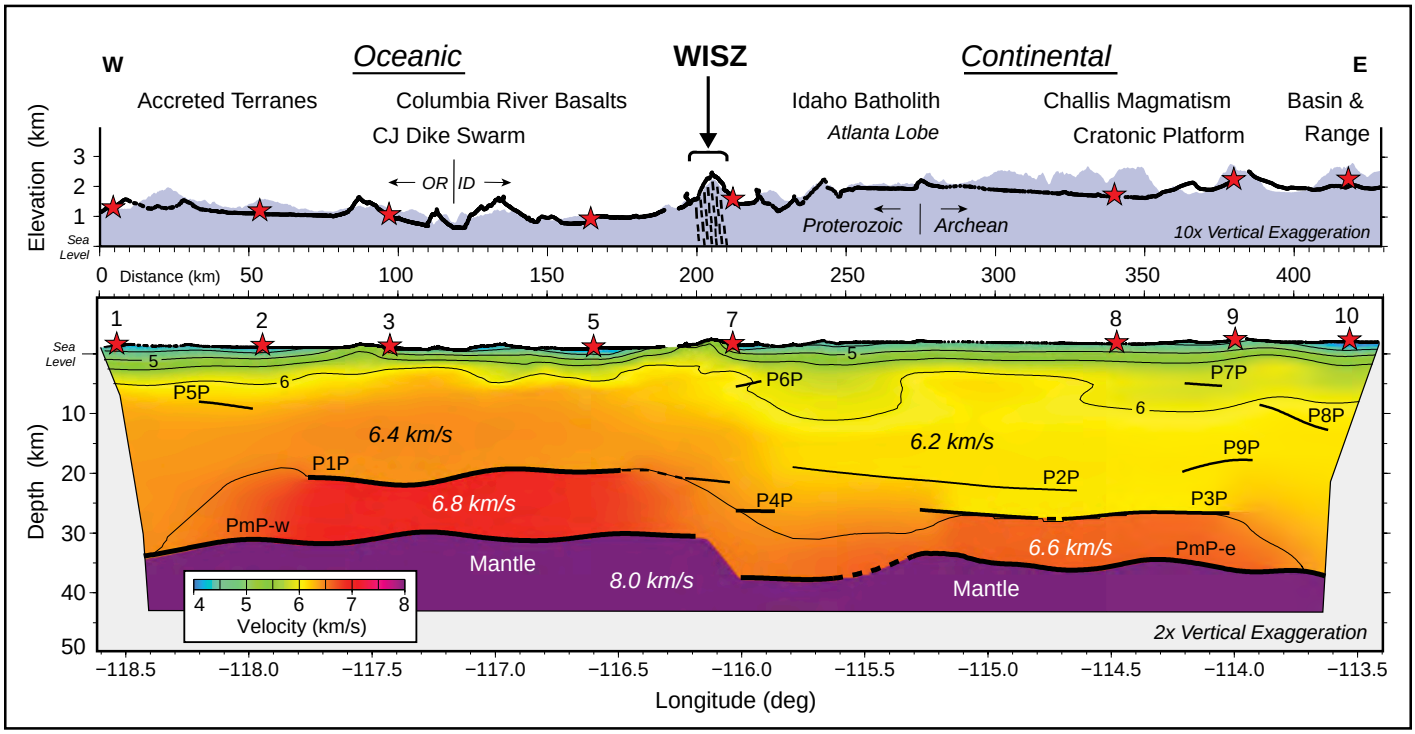

Figure 10. P-wave seismic velocity model and surface geology. (Bottom) Velocity contour interval is 0.5 km/s. Thick black lines mark the location of the seismic reflectors, dashed where not constrained. Vertical exaggeration is 2:1. (Top) Elevation averaged in a swath ±5 km from 44.5°N, from Shuttle Radar Topography Mission (SRTM) data (Jarvis et al., 2008). Topography vertical exaggeration is 10:1. Station and shot elevations are along the crooked line. CJ Dike Swarm—Chief Joseph dike swarm; WISZ—western Idaho shear zone; OR—Oregon; ID—Idaho. The Proterozoic-Archean boundary shown is for inherited zircon cores in the Atlanta lobe of the Idaho batholith.

there was significant lateral variation. On the west under the accreted terranes, the Moho is 31–32 km below the land surface and deepens modestly toward the western end of the line (Fig. 10). The Moho beneath the batholith and craton is at 37–40 km depth below the higher-elevation land surface (Fig. 10). An ~7 km offset on the Moho exists within <15 km beneath the WISZ (Fig. 10).

The upper-mantle seismic velocity is constrained by the Pn arrivals. After ray tracing through the crust's strong lateral variations, the Pn traveltimes are consistent with ~8.0 km/s constant velocity along the entire line.

GEOLOGIC AND TECTONIC INTERPRETATION

Western Idaho Shear Zone

Analysis of the IDOR controlled-source seismic profile reveals the WISZ to be a through-going feature of the crust, indicating that the juxtaposition of oceanic- and continental-affinity rocks extends in a near-vertical orientation through the entire crust, at least to the depth of the Moho and possibly deeper into the lithosphere (Figs. 9 and 10). At the surface, the steeply dipping WISZ represents the boundary that separates relatively young oceanic-island-arc terranes of the Blue Mountains Province from the Precambrian North American craton and Idaho batholith (e.g., McClelland et al., 2000; Tikoff et al., 2001; Giorgis et al., 2008). We determine that this strong contrast in terrane age and composition extends throughout the entire crust, manifested as changes in the seismic character and contrasting seismic wave speeds observed on either side of the shear zone (Figs. 9 and 10). Below the surface expression of the WISZ, the PmP reflections are not well constrained for a distance of <15 km between the shallower western and deeper eastern portions of the Moho. This gap begins directly beneath the WISZ and extends eastward under Long Valley (Fig. 10). This location is consistent with surface mapping of the WISZ, which indicates a current dip of 70°–80° to the east, while estimates of Miocene-to-modern extension restore the boundary to near-vertical prior to the Miocene (Tikoff et al., 2001). The contrasting crustal seismic velocities, the sharp Moho offset, and the coincidence of these features with the surface WISZ indicate that the WISZ is a through-going crustal boundary.

Transpressional deformation on the WISZ resulted in significant tectonic shortening of the broad Salmon River suture zone between the accreted terranes and craton (e.g., Giorgis et al., 2005), resulting in a very narrow boundary between oceanic and continental geochemical signatures across the WISZ (Armstrong et al., 1977; Fleck and Criss, 1985; Manduca et al., 1993). Syn–WISZ continental-arc plutons record an unusually narrow $^{87}Sr/^{86}Sr$ isotopic break coincident with the WISZ, indicating a steep boundary between oceanic and continental source rocks to at least the lower crust. A similarly sharp Sr isotope transition was observed in Miocene volcanic rocks ~120–150 km to the west of the WISZ in eastern Oregon, indicating a similar steep boundary in the lithospheric upper mantle (Hart, 1985; Leeman et al., 1992; Evans et al., 2002). Based on the differing depths of the source rocks, the dual steep ocean/continent boundaries were interpreted as evidence for a "shelf" of continental lithosphere extending west beneath the oceanic terranes visible at the surface (Fig. 2; Leeman et al., 1992). The top of this shelf was hypothesized to be a younger detachment crosscutting the WISZ and related to Sevier orogeny deformation far inboard. Our seismic image indicates that the WISZ extends steeply through the entire crust, and no detachment crosscuts it

within the crust or at the Moho. Subhorizontal ductile detachments often produce strong seismic reflections, but none was observed in the IDOR data beneath the Moho. If compression was transmitted inboard via a horizontal detachment, it must be deeper in the mantle.

The strong contrast in age, composition, and rheology between the oceanic accreted terranes and the cratonic lithosphere had a significant influence on tectonic processes since 90 Ma. Post–WISZ granitic plutons of the Idaho batholith were emplaced close to the shear zone on the cratonic side (Fig. 1) and appear to be the result of melting in a thickened crust (Gaschnig et al., 2011; Byerly et al., 2016; Fayon et al., 2017). The lack of widespread intracrustal melting west of the shear zone implies a preferential susceptibility in the cratonic crust, probably due to greater thickness and the lower temperature required to melt more felsic rocks.

Miocene extension associated with the Columbia River Basalts is pervasive west of the WISZ (e.g., Camp and Ross, 2004; Hooper et al., 2007; Camp, 2013). The feeder dike system for the Columbia River Basalt volcanics is widespread in the accreted terranes and only crosses the WISZ in small isolated locations (Fig. 1; Reidel et al., 2013b), although some surface flows extend more broadly east of the WISZ (Reidel et al., 2013a). Miocene-to-modern extension exists in easternmost Idaho, but only affects the Idaho batholith in isolated locations such as Long Valley, immediately to the east of the WISZ in the study area, where extension has tilted the WISZ from near vertical to its current steep 70°–80° eastward dip (Tikoff et al., 2001; Giorgis et al., 2006). This distribution of extensional features indicates that the thinner accreted terrane side of the boundary is more susceptible to extension than the more felsic crust east of the WISZ. The compartmentalization of magmatism and tectonic deformation to either side of the WISZ likely results from the juxtaposition of crustal architectures that respond independently to tectonic stresses and heating events due to significantly different composition, thickness, and deformation history. This effect demonstrates the importance of structural and rheological inheritance on the response of the crust to subsequent tectonic and magmatic events.

Blue Mountains Province Accreted Terranes

The accreted terranes observed in outcrops west of the WISZ consist of oceanic island arcs and intervening sedimentary basins (Vallier and Brooks, 1995; Dorsey and LaMaskin, 2007). The seismic velocities in this region (Figs. 9 and 10) are inferred to represent intermediate compositions from 5 to 7 km depth through the middle crust, consistent with other accreted oceanic-island-arc terranes in the North American Cordillera (e.g., Spence et al., 1985; Spence and Asudeh, 1993; Hammer and Clowes, 2004; Stephenson et al., 2011). Variations in the near-surface velocity are caused by local sedimentary basins associated with Cenozoic extensional valleys and by sedimentary units of the amalgamated terranes.

The crust in this region is ~32 km thick, and the Moho deepens toward the west. Crustal thickness of ~35 km at the west end of the line is consistent with that observed on controlled-source seismic data ~35 km to the west in the High Lava Plains (Cox et al., 2013). Broadband seismic data reveal a similar trend in crustal thickness across eastern Oregon and western Idaho (Eagar et al., 2011).

The thinnest crust in the IDOR controlled-source profile, ~31 km, occurs west of the WISZ near the Snake River at the boundary between Oregon and Idaho (Fig. 10). This area is where the line crosses the southern end of the Chief Joseph dike swarm, which fed the outpouring of Columbia River Basalt flows (Fig. 1; Reidel et al., 2013b). Wolff and Ramos (2013) identified this area as the primary source location for mantle upwelling that supplied a significant volume of the Columbia River Basalts via dikes that emerged in the massive Grande Ronde lava flows up to 400 km to the north. The seismic data include an unusually high-amplitude P1P reflection at this location (Fig. 3) from the top of an 8–10-km-thick, lower-crustal layer with ~6.8 km/s velocity (Figs. 9 and 10). We interpret the high-velocity lower-crustal layer beneath this strong seismic reflector (Fig. 10) as basaltic intrusion and/or underplating in the source region of the Columbia River Basalt basalts.

North American Craton

East of the WISZ, the Precambrian craton is 37–40 km thick, averaging ~5 km thicker than the accreted terrane crust west of the shear zone (Figs. 9 and 10). On the craton side, the velocity is slower compared to the accreted terranes and is interpreted to indicate felsic composition in the upper and middle crust and intermediate composition in the lower crust. Crust at all depths east of the WISZ has lower seismic velocity and is interpreted to be more felsic than average continental crust, while crust to the west is faster and therefore likely more mafic than average (Fig. 9; Christensen and Mooney, 1995). There is no significant difference in velocity between the Idaho batholith and the host cratonic blocks (Figs. 9 and 10).

The Idaho batholith extends approximately from the WISZ to the location of shot 8, with the dominant Atlanta lobe between approximately model km 225 and 320 on the seismic line (Figs. 1 and 10). Beneath the Atlanta lobe, the velocities are interpreted to indicate a felsic composition to >24 km depth below surface and are consistent with granite-granodiorite plutons and/or granitic metamorphic lithologies (Christensen and Mooney, 1995). Beneath the eastern half of the Atlanta lobe, the velocity gradient is slightly higher from 5 to 15 km depth compared to the adjacent batholith or craton. The cratonic platform east of the Idaho batholith is partially intruded by Challis magmatism at a shallow depth (Moye et al., 1988). We did not observe a velocity signature associated with the Challis plutons or volcanics. The eastern end of the seismic line crosses extensional valleys and ridges associated with the Basin and Range. Velocity in this region is similar to the western part of the craton and the Idaho batholith, consistent with felsic lithologies to ~28 km depth. Reflectors in this region could be detachments or other features related to Basin and Range extension. None of the reflectors imaged east of the WISZ exhibits a high amplitude or lateral extent consistent with a large-scale Sevier thrust detachment that could have offset the WISZ and transmitted Late Cretaceous compression into Montana and Wyoming.

A modest-amplitude reflector at 22–25 km subsurface depth correlates with the lateral extent of the Atlanta lobe, while a reflector at 28–29 km depth extends east from the center of the batholith and also underlies the unintruded craton (Fig. 10). The relative curvatures of the reflections from these features constrain the composition to be felsic below the western part of the Atlanta lobe at least to the depth of the shallower reflector at ~22 km, and to the depth of the deeper reflector at ~29 km beneath the eastern half of the Atlanta lobe. Where the two reflectors overlap laterally, the velocity between them must be as slow as above the shallower reflector. The relative curvatures of these reflections and the reflection from the Moho constrain the lower crust to have a faster average velocity; therefore, the composition is likely intermediate.

Beneath the deeper P3P reflector, the velocity average of the 8–10-km-thick layer above the Moho is 6.6 km/s, which is consistent with the P-wave velocity of diorite and in the range of velocities between felsic and mafic granulite (Christensen and Mooney, 1995). This velocity is not consistent with a mafic-to-ultramafic composition, such as mafic garnet granulite (Vp ~7.0 km/s) or eclogite (Vp ~7.9 km/s), which would be left behind by the melting of a mafic protolith in a continental arc (Beard and Lofgren, 1991; Rapp and Watson, 1995). The velocity and inferred

intermediate composition are consistent with a residual left by intracrustal melting of a felsic protolith. A velocity discontinuity is the preferred model for the P3P reflector based on the strength of the velocity contrast across the reflector.

Beneath the western Atlanta lobe, near the offset in the WISZ, the curvatures of the ~22 km P2P reflector and Moho reflections require an increase in the average velocity between 22 and 40 km depth. A velocity discontinuity is not required, since the data can be matched by either a layered zone or a gradient with the same average velocity. The deeper ~28–29 km P3P reflector and associated intermediate-composition layer could extend westward and connect to the P4P reflector at the WISZ step, but there is no evidence in the data to support this connection due to the shot and station gaps. If the P3P arrival is present on shot 7 at longer offsets, it is obscured by the P2P and PmP reflections; alternatively, it may be truly absent. Additionally, P4P has high-amplitude, near-zero offset and is not identifiable at >30 km offset. It would be very unusual for a reflection from the top of a strong velocity contrast to decrease in amplitude as it approaches the critical angle. For these reasons, the velocity between P2P and the Moho has been modeled without a velocity discontinuity, and P4P has been considered an independent reflector adjacent to the WISZ (Fig. 10).

Idaho Batholith

The mostly felsic to intermediate composition of the Idaho batholith is similar to other exhumed Cordilleran Cretaceous batholiths in the California Sierra Nevada and Peninsular Ranges, and the British Columbia Coast Mountains (Spence and McLean, 1998; Fliedner et al., 2000; Hammer et al., 2000; Morozov et al., 2003). These other batholiths, like the western border suite of the Idaho batholith, are predominantly metaluminous granodiorites, whereas the Atlanta and Bitterroot lobes are predominantly peraluminous mica granites. Subduction-related continental arc batholiths are typically formed by dehydration partial melting of a mafic protolith, leaving behind a pyroxene-enriched residual (Beard and Lofgren, 1991; Rapp and Watson, 1995). Lack of evidence for this residual beneath exhumed Cretaceous batholiths in North America has been interpreted as evidence that it was delaminated into the mantle (Kay and Mahlburg Kay, 1993). The granites of the Atlanta lobe are primarily crustal-source granites (Gaschnig et al., 2011), however, and do not necessitate the existence of a pyroxene-rich residual. We did not observe evidence of a pyroxene-rich residual in the lower crust beneath the Idaho batholith, which we interpret as further evidence that the Idaho batholith melted in a thickened crust.

The lateral extent of the reflector at ~22 km subsurface depth coincides with the surface extent of the Atlanta lobe of the Idaho batholith. Major- and trace-element geochemistry indicates that the Atlanta lobe melted in the garnet stability field of the lower crust, ≥35 km depth (Gaschnig et al., 2011). This reflector is roughly consistent with the minimum Late Cretaceous melting depth when ≥10 km of exhumation of the Idaho batholith (Fayon et al., 2017) is considered. Adding the estimated minimum exhumation to the current crustal thickness of 37–40 km yields a total crustal thickness of >50 km at the time of magmatism. This thickness is consistent with a thickened-crust melt source for the Idaho batholith, as proposed by Foster et al. (2001) for the northern Bitterroot lobe and by Gaschnig et al. (2011) for the Atlanta lobe, rather than a subduction-related arc source. Thickened crust is also consistent with observed petrographic fabrics (Byerley et al., 2016). The spatial extent, lack of velocity contrast, and low amplitude of the reflection from the ~22 km reflector are consistent with a structural or textural feature related to the formation of the batholith, rather than a velocity discontinuity. We interpret this reflector to be the top of the source zone of melting for the Atlanta lobe in a Late Cretaceous thickened crust. Melting of a felsic protolith produce a smaller volume of less-felsic residual than the melting of a mafic protolith. This residual could be distributed in the lower crust, represented by the underlying rocks interpreted as intermediate composition.

The source zone for melting of the Atlanta lobe was ≥35 km, but the relationship of the Atlanta lobe to plutons of the early metaluminous suite indicates the depth of emplacement was much shallower, in the mid-to-upper crust (Gaschnig et al., 2010), consistent with estimates of exhumation (Fayon et al., 2017). There is evidence that the Bitterroot lobe was emplaced in the crust as a relatively thin sill, because the floor of the batholith is exposed in a metamorphic dome (Vallier and Brooks, 1986). Beneath the Idaho batholith, the velocity and average crustal thickness are very similar to the unintruded craton to the east, leading to the possibility that the Atlanta lobe is also relatively thin and extends to <10 km current depth.

The lateral extent of the ~29-km-deep P3P reflector corresponds to the region of higher velocity gradient in the upper crust, and to a change in the depth of the Moho at the base of the crust (Figs. 9 and 10). These lateral changes in the velocity model are all coincident with the Archean-Proterozoic basement boundary at model km 275 ± 20 (Fig. 1) interpreted by Gaschnig et al. (2011) based on inherited zircon core data in Atlanta lobe plutons. We interpret the lateral change in crustal architecture beneath the center of the Atlanta lobe to be the northeastern margin of the Archean Grouse Creek craton. The continuity of crustal structure below the eastern surface boundary of the Idaho batholith combined with lateral contrasts at multiple depths in the crust at the interpreted Archean craton boundary indicate that the batholith has not strongly overprinted the crustal architecture of the preexisting craton.

CONCLUSIONS

Transpressional deformation in the WISZ formed a steep boundary between oceanic accreted terranes and the Precambrian North American craton. Traveltime inversion of the IDOR controlled-source seismic data indicates significant contrasts in velocity and crustal thickness that reveal the boundary to be a through-going feature of the crust that offsets the Moho ~7 km. This juxtaposition of crustal units with significantly different compositions, ages, strengths, and thicknesses provided a mechanism for preferential distribution of post–WISZ deformation and magmatism, leading to structural inheritance influencing subsequent tectonic events.

West of the steep boundary, the accreted terrane crust is ~32 km thick, with seismic velocities inferred to represent intermediate composition in the upper and middle crust, consistent with the oceanic-arc terranes. We interpret a high-velocity, 8–10-km-thick, lower-crustal layer to be a mafic magmatic intrusion and/or underplating associated with the Chief Joseph dike swarm feeder system of the Columbia River Basalt Group. On the eastern, cratonic side of the WISZ, the crust is 37–40 km thick. Slower seismic velocities that are interpreted as indicative of felsic lithologies persist to 25–28 km depth. There is not a significant difference in upper- and middle-crustal velocity below the granitic Idaho batholith and the unintruded craton to the east. A reflector at 22–25 km depth beneath the Atlanta lobe of the Idaho batholith is interpreted as the top of the zone of melting that fed the intrusion. Continuity of crustal architecture across the eastern margin of the Idaho batholith and a change of crustal architecture beneath the center of the batholith are interpreted to map the Archean Grouse Creek cratonic block extending beneath the batholith. Thick felsic-to-intermediate crust, combined with exhumation, indicates a Late Cretaceous crustal thickness of ≥50 km, which is consistent with the voluminous Atlanta lobe of the Idaho batholith forming by internal melting within a thickened crust.

ACKNOWLEDGMENTS

Data acquisition and analysis for this project were funded by National Science Foundation (NSF) EarthScope Program grants EAR-0844264 and EAR-1251724 to Virginia Tech, EAR-0844260 and EAR-1251877 to University of Wisconsin–Madison, and EAR-0844187 and EAR-1251814 to University of Florida. The seismic instruments were provided by the Incorporated Research Institutions for Seismology (IRIS) through the PASSCAL Instrument Center at New Mexico Tech. Data collected will be available through the IRIS Data Management Center. The facilities of the IRIS Consortium are supported by the NSF under Cooperative Agreement EAR-1261681 and the U.S. Department of Energy National Nuclear Security Administration. Special thanks go to George Slad for field management. We gratefully acknowledge the survey crew, shooter crew, and field crew, including ~45 student volunteers, who made the data acquisition possible, as well as the landowners and public land managers who supported the project. This research used software provided by Landmark Software and Services, a Halliburton Company. We wish to thank Richard Gaschnig, Annia Fayon, Christian Stanciu, Jeffrey Vervoort, Paul Kelso, and Paul Bremner for many helpful conversations that aided the interpretation.

REFERENCES CITED

Armstrong, R.L., and Ward, P., 1991, Evolving geographic patterns of Cenozoic magmatism in the North American Cordillera: The temporal and spatial association of magmatism and metamorphic core complexes: Journal of Geophysical Research, v. 96, p. 13,201–13,224, doi:10.1029/91JB00412.

Armstrong, R.L., Taubeneck, W.H., and Hales, P.O., 1977, Rb-Sr and K-Ar geochronometry of Mesozoic granitic rocks and their Sr isotopic composition, Oregon, Washington, and Idaho: Geological Society of America Bulletin, v. 88, p. 397–411, doi:10.1130/0016-7606(1977)88<397.

Beard, J.S., and Lofgren, G.E., 1991, Dehydration melting and water-saturated melting of basaltic and andesitic greenstones and amphibolites at 1, 3, and 6. 9 kb: Journal of Petrology, v. 32, no. 2, p. 365–401, doi:10.1093/petrology/32.2.365.

Benford, B., Crowley, J., Schmitz, M., Northrup, C.J., and Tikoff, B., 2010, Mesozoic magmatism and deformation in the Owyhee Mountains, Idaho: Implications for along-strike variations in the western Idaho shear zone: Lithosphere, v. 2, p. 93–118, doi:10.1130/L76.1.

Bennett, E.H., 1986, Relationship of the trans-Challis fault system in central Idaho to Eocene and Basin and Range extensions: Geology, v. 14, no. 6, p. 481–484, doi:10.1130/0091-7613(1986)14<481:ROTTFS>2.0.CO;2.

Blake, D.E., Gray, K.D., Giorgis, S., and Tikoff, B., 2009, A tectonic transect through the Salmon River suture zone along the Salmon River Canyon in the Riggins region of west- central Idaho, *in* O'Conner, J.E., Dorsey, R.J., and Madin, I.P., eds., Volcanoes to Vineyards: Geologic Field Trips through the Dynamic Landscape of the Pacific Northwest: Geological Society of America Annual Meeting Field Trip Guide 15, p. 345–372, doi:10.1130/2009.fld015(18).

Bond, G.C., Nickerson, P.A., and Kominz, M.A., 1984, Breakup of a supercontinent between 625 Ma and 555 Ma: New evidence and implications for continental histories: Earth and Planetary Science Letters, v. 70, p. 325–345, doi:10.1016/0012-821X(84)90017-7.

Braudy, N., Gaschnig, R., Wilford, D., Vervoort, J., Nelson, C.L., Davidson, C., Kahn, M.J., and Tikoff, B., 2016, Timing and deformation conditions of the western Idaho shear zone, West Mountain, west-central Idaho: Lithosphere, doi:10.1130/L519.1.

Brooks, H.C., 1979, Geologic Map of Huntington and Part of Olds Ferry Quadrangles, Oregon: Oregon Department of Geology and Mineral Industries Geologic Map Series GMS-13, scale 1:62,500.

Byerly, A., Tikoff, B., Kahn, M.J., Jicha, B., and Gaschnig, R., 2016, Internal fabrics of the Idaho batholith, USA: Lithosphere, doi:10.1130/L551.1.

Camp, V.E., 2013, Origin of Columbia River Basalt: Passive rise of shallow mantle, or active upwelling of a deep-mantle plume?, *in* Reidel, S.P., Camp, V.E., Ross, M.E., Wolff, J.A., Martin, B.S., Tolan, T.L., and Wells, R.E., eds., The Columbia River Flood Basalt Province: Geological Society of America Special Paper 497, p. 181–199, doi:10.1130/2013.2497(07).

Camp, V.E., and Ross, M.E., 2004, Mantle dynamics and genesis of mafic magmatism in the Intermontane Pacific Northwest: Journal of Geophysical Research, v. 109, no. B8, B08204, doi:10.1029/2003JB002838.

Christensen, N.I., 1996, Poisson's ratio and crustal seismology: Journal of Geophysical Research, v. 101, p. 3139–3156, doi:10.1029/95JB03446.

Christensen, N.I., and Mooney, W.D., 1995, Seismic velocity structure and composition of the continental crust: A global view: Journal of Geophysical Research, v. 100, p. 9761–9788, doi:10.1029/95JB00259.

Cox, C., Keller, G.R., and Harder, S.H., 2013, A controlled-source seismic and gravity study of the High Lava Plains (HLP) of eastern Oregon: Geochemistry Geophysics Geosystems, v. 14, p. 5208–5226, doi:10.1002/2013GC004870.

Dickinson, W., 1979, Mesozoic forearc basin in central Oregon: Geology, v. 7, p. 166–170, doi:10.1130/0091-7613(1979)7<166:MFBICO>2.0.CO;2.

Dickinson, W., 2004, Evolution of the North American Cordillera: Annual Review of Earth and Planetary Sciences, v. 32, p. 13–45, doi:10.1146/annurev.earth.32.101802.120257.

Dorsey, R., and LaMaskin, T., 2007, Stratigraphic record of Triassic-Jurassic collisional tectonics in the Blue Mountains Province, northeastern Oregon: American Journal of Science, v. 307, p. 1167–1193, doi:10.2475/10.2007.03.

Eagar, K.C., Fouch, M.J., James, D.E., and Carlson, R.W., 2011, Crustal structure beneath the High Lava Plains of eastern Oregon and surrounding regions from receiver function analysis: Journal of Geophysical Research, v. 116, B02313, doi:10.1029/2010JB007795.

Evans, J.G., Griscom, A., Halvorsom, P.F., and Cummings, M.L., 2002, Tracking the western margin of the North American craton beneath southeastern Oregon: A multidisciplinary approach, *in* Bonnichsen, B., White, C.M., and McCurry, M., eds., Tectonic and Magmatic Evolution of the Snake River Plain Volcanic Province: Idaho Geological Survey Bulletin 30, p. 35–57.

Fayon, A.K., Tikoff, B., Kahn, M., and Gaschnig, R.M., 2017, Cooling and exhumation of the southern Idaho batholith: Lithosphere, doi:10.1130/L565.1.

Fleck, R.J., and Criss, R.E., 1985, Strontium and oxygen isotopic variations in Mesozoic and Tertiary plutons of central Idaho: Contributions to Mineralogy and Petrology, v. 90, p. 291–308, doi:10.1007/BF00378269.

Fliedner, M.M., Klemperer, S.L., and Christensen, N.I., 2000, Three-dimensional seismic model of the Sierra Nevada arc, California, and its implications for crustal and upper mantle composition: Journal of Geophysical Research, v. 105, p. 10,899–10,921, doi:10.1029/2000JB900029.

Foster, D.A., Schafer, C., Fanning, C.M., and Hyndman, D.W., 2001, Relationships between crustal partial melting, plutonism, orogeny, and exhumation: Idaho–Bitterroot batholith: Tectonophysics, v. 342, p. 313–350, doi:10.1016/S0040-1951(01)00169-X.

Foster, D.A., Mueller, P.A., Mogk, D.W., Wooden, J.L., and Vogl, J.J., 2006, Proterozoic evolution of the western margin of the Wyoming craton: Implications for the tectonic and magmatic evolution of the northern Rocky Mountains: Canadian Journal of Earth Sciences, v. 43, p. 1601–1619, doi:10.1139/e06-052.

Gaschnig, R.M., Vervoort, J.D., Lewis, R.S., and McClelland, W.C., 2010, Migrating magmatism in the northern US Cordillera: In situ U-Pb geochronology of the Idaho batholith: Contributions to Mineralogy and Petrology, v. 159, p. 863–883, doi:10.1007/s00410-009-0459-5.

Gaschnig, R.M., Vervoort, J.D., Lewis, R.S., and Tikoff, B., 2011, Isotopic evolution of the Idaho batholith and Challis intrusive province, northern US Cordillera: Journal of Petrology, v. 52, p. 2397–2429, doi:10.1093/petrology/egr050.

Gaschnig, R.M., Vervoort, J.D., Lewis, R.S., and Tikoff, B., 2013, Probing for Proterozoic and Archean crust in the northern U.S. Cordillera with inherited zircon from the Idaho batholith: Geological Society of America Bulletin, v. 125, p. 73–88, doi:10.1130/B30583.1.

Gaschnig, R.M., Vervoort, J.D., Tikoff, B., and Lewis, R.S., 2016, Construction and preservation of batholiths in the northern U.S. Cordillera: Lithosphere, doi:10.1130/L497.1.

Gehrels, G.E., 2001, Geology of the Chatham Sound region, southeast Alaska and coastal British Columbia: Canadian Journal of Earth Sciences, v. 38, p. 1579–1599, doi:10.1139/e01-040.

Getty, S.R., Selverstone, J., Wernicke, B.P., Jacobsen, S.B., Aliberti, E., and Lux, D.R., 1993, Sm-Nd dating of multiple garnet growth events in an arc-continent collision zone, northwestern U.S. Cordillera: Contributions to Mineralogy and Petrology, v. 115, p. 45–57, doi:10.1007/BF00712977.

Giorgis, S., Tikoff, B., and McClelland, W., 2005, Missing Idaho arc: Transpressional modification of the $^{87}Sr/^{86}Sr$ transition on the western edge of the Idaho batholith: Geology, v. 33, p. 469–472, doi:10.1130/G20911.1.

Giorgis, S., Tikoff, B., Kelso, P., and Markley, M., 2006, The role of material anisotropy in the neotectonic extension of the western Idaho shear zone, McCall, Idaho: Geological Society of America Bulletin, v. 118, no. 3–4, p. 259–273, doi:10.1130/B25382.1.

Giorgis, S., McClelland, W., Fayon, A., Singer, B.S., and Tikoff, B., 2008, Timing of deformation and exhumation in the western Idaho shear zone, McCall, Idaho: Geological Society of America Bulletin, v. 120, p. 1119–1133, doi:10.1130/B26291.1.

Giorgis, S., Michels, Z., Dair, L., Braudy, N., and Tikoff, B., 2016, Kinematic and vorticity analyses of the western Idaho shear zone, USA: Lithosphere, doi:10.1130/L518.1.

Gray, K.D., and Oldow, J.S., 2005, Contrasting structural histories of the Salmon River belt and Wallowa terrane: Implications for terrane accretion in northeastern Oregon and west-central Idaho: Geological Society of America Bulletin, v. 117, p. 687–706, doi:10.1130/B25411.1.

Hamilton, W.R., 1963, Metamorphism in the Riggins Region, Western Idaho: U.S. Geological Survey Professional Paper 436, 95 p.

Hammer, P.T.C., and Clowes, R.M., 2004, Accreted terranes of northwestern British Columbia, Canada: Lithospheric velocity structure and tectonics: Journal of Geophysical Research, v. 109, B06305, doi:10.1029/2003JB002749.

Hammer, P.T.C., Clowes, R.M., and Ellis, R.M., 2000, Crustal structure of NW British Columbia and SE Alaska from seismic wide-angle studies: Coast Plutonic Complex to Stikinia: Journal of Geophysical Research, v. 105, p. 7961–7981, doi:10.1029/1999JB900378.

Harder, S., Miller, K., and Snelson, C., 2011, The relative effect on charge configuration on seismic amplitudes, *in* Proceedings of the 2011 Monitoring Research Review Meeting: Ground-Based Nuclear Explosion Monitoring Technologies, Tucson, Arizona, 13–15 September 2011, p. 467–472.

Hart, W.K., 1985, Chemical and isotopic evidence for mixing between depleted and enriched mantle, northwestern U.S.A.: Geochimica et Cosmochimica Acta, v. 49, p. 131–144, doi:10.1016/0016-7037(85)90197-8.

Hole, J.A., 1992, Nonlinear high-resolution three-dimensional seismic travel time tomography: Journal of Geophysical Research, v. 97, p. 6553–6562, doi:10.1029/92JB00235.

Hole, J.A., and Zelt, B.C., 1995, 3-D finite-difference reflection traveltimes: Geophysical Journal International, v. 121, p. 427–434, doi:10.1111/j.1365-246X.1995.tb05723.x.

Hooper, P.R., Camp, V.E., Reidel, S.P., and Ross, M.E., 2007, The origin of the Columbia River flood basalt province: Plume versus nonplume models, *in* Foulger, G.R., and Jurdy, D.M., eds., Plates, Plumes and Planetary Processes: Geological Society of America Special Paper 430, p. 635–668, doi:10.1130/2007.2430(30).

Housen, B.A., and Dorsey, R.J., 2005, Paleomagnetism and tectonic significance of Albian and Cenomanian turbidites, Ochoco Basin, Mitchell Inlier, central Oregon: Journal of Geophysical Research, v. 110, B07102, doi:10.1029/2004JB003458.

Hyndman, D.W., 1983, The Idaho batholith and associated plutons, Idaho and western Montana, *in* Roddick, J.A., ed., Circum-Pacific Plutonic Terranes: Geological Society of America Memoir 159, p. 213–240, doi:10.1130/MEM159-p213.

Jarvis, A., Reuter, H.I., Nelson, A., and Guevara, E., 2008, Hole-filled seamless SRTM data V4: International Centre for Tropical Agriculture (CIAT), available from http://srtm.csi.cgiar.org (accessed July 2015).

Kay, R.W., and Mahlburg Kay, S., 1993, Delamination and delamination magmatism: Tectonophysics, v. 219, p. 177–189, doi:10.1016/0040-1951(93)90295-U.

LaMaskin, T.A., Vervoort, J.D., Dorsey, R.J., and Wright, J.E., 2011, Early Mesozoic paleogeography and tectonic evolution of the western United States: Insights from detrital zircon U-Pb geochronology, Blue Mountains Province, northeastern Oregon: Geological Society of America Bulletin, v. 123, p. 1939–1965, doi:10.1130/B30260.1.

LaMaskin, T.A., Dorsey, R.J., Vervoort, J.D., Schmitz, M.D., Tumpane, K.P., and Moore, N.O., 2015, Westward growth of Laurentia by pre–Late Jurassic terrane accretion, eastern Oregon and western Idaho, United States: The Journal of Geology, v. 123, p. 233–267, doi:10.1086/681724.

Leeman, W.P., Oldow, J.S., and Hart, W.K., 1992, Lithosphere-scale thrusting in the western U.S. Cordillera as constrained by Sr and Nd isotopic transitions in Neogene volcanic rocks: Geology, v. 20, p. 63–66, doi:10.1130/0091-7613(1992)020<0063:LSTITW>2.3.CO;2.

Lewis, R.S., and Kiilsgaard, T.H., 1991, Eocene plutonic rocks in south central Idaho: Journal of Geophysical Research, v. 96, p. 295–311, doi:10.1029/91JB00601.

Lewis, R.S., Link, P.K., Stanford, L.R., and Long, S.P., 2012, Geologic Map of Idaho: Idaho Geological Survey Geologic Map 9, scale 1:750,000.

Lund, K., and Snee, W.L., 1988, Metamorphism, structural development, and age of the continent–island arc juncture in west-central Idaho, *in* Ernst, W.G., ed., Metamorphism and Crustal Evolution of the Western United States, Rubey Volume VII: Englewood Cliffs, New Jersey, Prentice-Hall, p. 296–331.

Manduca, C.A., Kuntz, M.A., and Silver, L.T., 1993, Emplacement and deformation history of the western margin of the Idaho batholith near McCall, Idaho: Influence of a major terrane boundary: Geological Society of America Bulletin, v. 105, p. 749–765, doi:10.1130/0016-7606(1993)105<0749:EADHOT>2.3.CO;2.

McClelland, W.C., and Oldow, J.S., 2007, Late Cretaceous truncation of the western Idaho shear zone in the central North American Cordillera: Geology, v. 35, p. 723–726, doi:10.1130/G23623A.1.

McClelland, W.C., Tikoff, B., and Manduca, C.A., 2000, Two-phase evolution of accretionary margins: Examples from the North American Cordillera: Tectonophysics, v. 326, p. 37–55, doi:10.1016/S0040-1951(00)00145-1.

Morozov, I.B., Christensen, N.I., Smithson, S.B., and Hollister, L.S., 2003, Seismic and laboratory constraints on crustal formation in a former continental arc (ACCRETE, southeastern Alaska and western British Columbia): Journal of Geophysical Research, v. 108, p. 2041, doi:10.1029/2001JB001740.

Moye, F.J., Hackett, W.R., Blakley, J.D., and Snider, L.G., 1988: Regional Geologic Setting and Volcanic Stratigraphy of the Challis Volcanic Field, Central Idaho: Idaho Geologic Survey Bulletin 27, p. 87–98.

Oldow, J.S., Bally, A.W., Avé Lallemant, H.G., and Leeman, W.P., 1989, Phanerozoic evolution of the North American Cordillera, United States and Canada, *in* Bally, A.W., and Palmer, A.R., eds., The Geology of North America—An Overview: Boulder, Colorado, Geological Society of America, Geology of North America, v. A, p. 139–232.

Parsons, T., McCarthy, J., Kohler, W.M., Ammon, C.J., Benz, H.M., Hole, J., and Criley, E.E., 1996, Crustal structure of the Colorado Plateau, Arizona: Application of new long offset seismic data analysis techniques: Journal of Geophysical Research, v. 101, p. 11,173–11,194, doi:10.1029/95JB03742.

Rapp, R.P., and Watson, E.B., 1995, Dehydration melting of metabasalt at 8–32 kbar: Implications for continental growth and crust-mantle recycling: Journal of Petrology, v. 36, p. 891–931, doi:10.1093/petrology/36.4.891.

Reidel, S.P., and Hooper, P.R., eds., 1989, Volcanism and Tectonism in the Columbia River Flood-Basalt Province: Geological Society of America Special Paper 239, 386 p.

Reidel, S.P., Camp, V.E., Tolan, T.L., and Martin, B.S., 2013a, The Columbia River flood basalt province: Stratigraphy, areal extent, volume, and physical volcanology, *in* Reidel, S.P., Camp, V.E., Ross, M.E., Wolff, J.A., Martin, B.S., Tolan, T.L., and Wells, R.E., eds., The Columbia River Flood Basalt Province: Geological Society of America Special Paper 497, p. 1–43.

Reidel, S.P., Camp, V.E., Tolan, T.L., Kauffman, J.D., and Garwood, D.L., 2013b, Tectonic evolution of the Columbia River flood basalt province, *in* Reidel, S.P., Camp, V.E., Ross, M.E., Wolff, J.A., Martin, B.S., Tolan, T.L., and Wells, R.E., eds., The Columbia River Flood Basalt Province: Geological Society of America Special Paper 497, p. 293–324.

Schwartz, J.J., Johnson, K., Miranda, E.A., and Wooden, J.L., 2011, The generation of high Sr/Y plutons following Late Jurassic arc-arc collision, Blue Mountains Province, NE Oregon: Lithos, v. 126, p. 22–41, doi:10.1016/j.lithos.2011.05.005.

Selverstone, J., Wernicke, B.P., and Aliberti, E.A., 1992, Intracontinental subduction and hinged unroofing along the Salmon River suture zone, western central Idaho: Tectonics, v. 11, p. 124–144, doi:10.1029/91TC02418.

Spence, G.D., and Asudeh, I., 1993, Seismic velocity structure of the Queen Charlotte Basin beneath Hecate Strait: Canadian Journal of Earth Sciences, v. 30, p. 787–805, doi:10.1139/e93-065.

Spence, G.D., and McLean, N.A., 1998, Crustal seismic velocity and density structure of the Intermontane and Coast belts, southwestern Cordillera: Canadian Journal of Earth Sciences, v. 35, p. 1362–1379, doi:10.1139/e98-070.

Spence, G.D., Clowes, R.M., and Ellis, R.M., 1985, Seismic structure across the active subduction zone of western Canada: Journal of Geophysical Research, v. 90, p. 6754–6772, doi:10.1029/JB090iB08p06754.

Stanciu, A.C., Russo, R.M., Mocanu, V.I., Bremner, P.M., Hongsresawat, S., Torpey, M.E., VanDecar, J.C., Foster, D.A., and Hole, J.A., 2016, Crustal structure beneath the Blue Mountains terranes and cratonic North America, eastern Oregon, and Idaho, from teleseismic receiver functions: Journal of Geophysical Research, v. 121, p. 5049–5067, doi:10.1002/2016JB012989.

Stephenson, A.L., Spence, G.D., Wang, K., Hole, J.A., Miller, K.C., Clowes, R.M., Harder, S.H., and Kaip, G.M., 2011, Crustal velocity structure of the southern Nechako basin, British Columbia, from wide-angle seismic traveltime inversion: Canadian Journal of Earth Sciences, v. 48, p. 1050–1063, doi:10.1139/e11-006.

Tikoff, B., Kelso, P., Manduca, C., Markley, M.J., and Gillaspy, J., 2001, Lithospheric and crustal reactivation of an ancient plate boundary: The assembly and disassembly of the Salmon River suture zone, Idaho, USA, *in* Holdsworth, R.E., Strachan, R.A., and Magloughlin, J.F., eds., Fault Reactivation: Geological Society, London, Special Publication 186, p. 213–231, doi:10.1144/GSL.SP.2001.186.01.13.

Tikoff, B., Benford, B., and Giorgis, S., 2008, Lithospheric control on the initiation of the Yellowstone hotspot: Chronic reactivation of lithospheric scars: International Geology Review, v. 50, p. 305–324, doi:10.2747/0020-6814.50.3.305.

Tikoff, B., Vervoort, J., Hole, J.A., Russo, R., Gaschnig, R., and Fayon, A., 2017, Introduction: EarthScope IDOR project (Deformation and Magmatic Modification of a Steep Continental Margin, Western Idaho–Eastern Oregon) Themed Issue: Lithosphere, doi:10.1130/L628.1.

Vallier, T.L., 1977, The Permian and Triassic Seven Devils Group, Western Idaho and Northeastern Oregon: U.S. Geological Survey Bulletin 1437, 68 p.

Vallier, T.L., and Brooks, H.C., 1986, Geology of the Blue Mountains Region of Oregon, Idaho, and Washington: Geologic Implications of Paleozoic and Mesozoic Paleontology and Biostratigraphy, Blue Mountains Province, Oregon and Idaho: U.S. Geological Survey Professional Paper 1435, p. 1–9.

Vallier, T.L., and Brooks, H.C., eds., 1995, Geology of the Blue Mountains Region of Oregon, Idaho, and Washington: Petrology and Tectonic Evolution of Pre-Tertiary Rocks of the Blue Mountains Region: U.S. Geological Survey Professional Paper 1438, 540 p.

Vidale, J.E., 1990, Finite-difference calculation of traveltimes in three dimensions: Geophysics, v. 55, p. 521–526, doi:10.1190/1.1442863.

Waters, A.C., 1961, Stratigraphic and lithologic variations in the Columbia River Basalt: American Journal of Science, v. 259, p. 583–611, doi:10.2475/ajs.259.8.583.

Wolff, J.A., and Ramos, F.C., 2013, Source materials for the main phase of the Columbia River Basalt Group: Geochemical evidence and implications for magma storage and transport, *in* Reidel, S.P., Camp, V.E., Ross, M.E., Wolff, J.A., Martin, B.S., Tolan, T.L., and Wells, R.E., eds., The Columbia River Flood Basalt Province: Geological Society of America Special Paper 497, p. 273–291, doi:10.1130/2013.2497(11).

Wyld, S.J., and Wright, J.E., 2001, New evidence for Cretaceous strike-slip faulting in the United States Cordillera and implications for terrane-displacement, deformation patterns, and plutonism: American Journal of Science, v. 301, p. 150–181, doi:10.2475/ajs.301.2.150.

Zelt, B.C., Ellis, R.M., Clowes, R.M., and Hole, J.A., 1996, Inversion of three-dimensional wide-angle seismic data from the southwestern Canadian Cordillera: Journal of Geophysical Research, v. 101, p. 8503–8529, doi:10.1029/95JB02807.

Zelt, C.A., 1999, Modeling strategies and model assessment for wide-angle seismic traveltime data: Geophysical Journal International, v. 139, p. 183–204, doi:10.1046/j.1365-246X.1999.00934.x.

MANUSCRIPT RECEIVED 14 APRIL 2016
REVISED MANUSCRIPT RECEIVED 11 OCTOBER 2016
MANUSCRIPT ACCEPTED 22 DECEMBER 2016

Printed in the USA